JOURNAL OF SOLID STATE CHEMISTRY 50, 281–293 (1983)

Magnetic Properties of the Semiconducting Lanthanide Cuprates Ln_2CuO_4 and Their Interpretation: Evidence for a New Series of Planar Copper Antiferromagnets*

R. SAEZ PUCHE

Departmento de Quimica Inorgánica, Facultad de Ciencias Químicas, Universidad Complutense, Madrid-3, Spain

AND M. NORTON, T. R. WHITE, AND W. S. GLAUNSINGER†

Department of Chemistry, Arizona State University, Tempe, Arizona 85287

Received January 20, 1983

The magnetic susceptibility of the semiconducting lanthanide cuprates Nd_2CuO_4, Pr_2CuO_4, Eu_2CuO_4, and Sm_2CuO_4 has been measured in the range 4–300 K. Below 300 K, the Cu^{2+} ions are ordered antiferromagnetically in the CuO_2 planes of these compounds, and the exchange interactions involving the Ln^{3+} ions are relatively weak. The suceptibility of the Ln^{3+} ions obeys the Curie–Weiss law at elevated temperatures, but deviations from this law occur at lower temperatures. An attempt is made to account for these deviations by fitting theoretical expressions for the susceptibility of isolated Ln^{3+} ions under the influence of a cubic crystal field to the experimental data. Excellent agreement is obtained for Nd^{3+} and Eu^{3+} over the entire temperature range and for Pr^{3+} and Sm^{3+} at elevated temperatures. Deviations at lower temperatures for the latter two ions may be due to structural changes, exchange interactions involving the Ln^{3+} ions, or possibly oxygen nonstoichiometry. The susceptibility parameters derived by fitting the theoretical expressions to the experimental data are also discussed. It is concluded that these compounds form an interesting new series of planar Cu^{2+}-ion antiferromagnets.

Introduction

Stimulated by the interest in magnetic films and critical phenomena, two-dimensional (2D) magnetic systems have been intensively studied in recent years. Several compounds having the general formula A_2BX_4, where A is a larger diamagnetic ion ($1.0 < r_A < 1.9$ Å), B is a smaller paramagnetic ion ($0.5 < r_B < 1.2$ Å), and X = O, F, or Cl, exhibit planar magnetic interactions. Many of these compounds adopt the tetragonal K_2NiF_4 structure shown in Fig. 1. This structure can be visualized as containing alternating perovskite (ABX_3) and rock-salt (AX) blocks, which results in nine-coordination for A and octahedral coordination for B. It is the relatively strong B–X–B superexchange interactions in the BX_2 planes of the perovskite layers that produces a 2D magnetically layered system (*1*).

The lanthanide cuprates, Ln_2CuO_4, with Ln^{3+} = La^{3+}, Pr^{3+}, Nd^{3+}, Sm^{3+}, Eu^{3+}, and

* This research was supported by Grants DMR 79-21069, 8006971, and 82-15315 from the National Science Foundation and a Spanish-American Grant to Dr. R. Saez Puche.

† To whom correspondence should be addressed.

0022-4596/83 $3.00

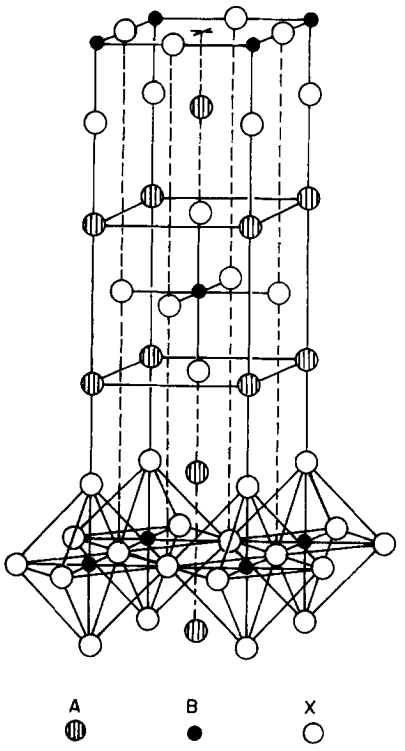

FIG. 1. The tetragonal K_2NiF_4 structure of A_2BX_4.

Gd^{3+}, provide interesting examples of A_2BX_4-type compounds. In this series the Ln^{3+} can be either diamagnetic (La^{3+}) or paramagnetic (Pr^{3+}, Nd^{3+}, Sm^{3+}, Eu^{3+}, and Gd^{3+}), so that it should be possible to determine the influence of the magnetic nature of Ln^{3+} on the planar Cu^{2+}–O^{2}–Cu^{2+} superexchange interaction. Although La_2CuO_4 crystallizes with a small orthohombic distortion of the ideal K_2NiF_4 structure, this compound is metallic due to the delocalization of the unpaired electron on Cu^{2+} in a conduction band, as indicated by electrical transport (*2, 3*) magnetic susceptibility (χ) (*4, 5*) and electron paramagnetic resonance (EPR) experiments (*5*). Electrical transport measurements (*2, 3, 6*) show that the other Ln_2CuO_4 compounds are *n*-type semiconductors, which probably originates from the partial decomposition of Cu^{2+} to Cu^{+}, corresponding to a small oxygen deficiency. The observation that the activation energy for electrical conduction at high temperatures ($E_a \approx 0.04$ eV) is nearly independent of the nature of *Ln* suggests that conduction occurs primarily by a thermally activated process within the CuO_2 planes, so that the resistivity should be highly anisotropic. However, these compounds apparently do not adopt the K_2NiF_4 structure. Recent single-crystal X-ray diffraction studies of Nd_2CuO_4 (*7*) and Gd_2CuO_4 (*8*) indicate that they crystallize in a new structure depicted in Fig. 2, in which Cu^{2+} exhibits square-planar, rather than octahedral, coordination to oxygen and Ln^{3+} is coordinated to eight, rather than nine, oxygen ligands.

In principle, the semiconducting Ln_2CuO_4 compounds could be magnetically very complex, since, in addition to the Cu^{2+}–O^{2-}–Cu^{2+} superexchange interaction, there exists the possibility of Cu^{2+}–O^{2-}–Ln^{3+} and Ln^{3+}–O^{2-}–Ln^{3+} superexchange pathways. However, in a previous study (*9*) we have found that Pr_2CuO_4, Nd_2CuO_4, and Gd_2CuO_4 obey the Curie–Weiss law, $\chi = C/(T - \theta)$, where $C = N\mu^2/3k$, above about 65, 30, and 10 K, respectively, and that the experimental magnetic moments are in good agreement with the calculated moments of Ln^{3+} and also with those of the corresponding lanthanide trifluorides (*10*) given in Table I. These results indicate that the Cu^{2+} ions are ordered antiferromagneti-

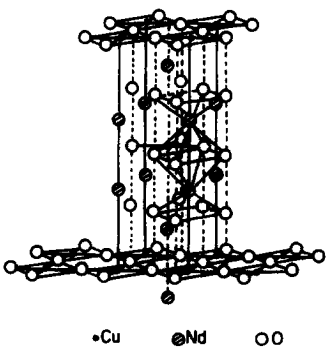

FIG. 2. The structure of Nd_2CuO_4 or Gd_2CuO_4.

cally below 300 K and that the exchange interactions involving the Ln^{3+} ions are relatively weak. In Gd_2CuO_4, a maximum in χ occurs near 5 K, which suggests that the Gd^{3+} moments have ordered antiferromagnetically, with the Néel temperature $T_N \approx 5$ K. This suggestion is supported by electron paramagnetic resonance measurements on this compound, which indicate that the Néel temperature is about 3 K. It was also noted that the deviations from the Curie–Weiss law for Pr_2CuO_4 and Nd_2CuO_4 were in qualitative agreement with the predicted behavior for isolated Ln^{3+} under the influence of a cubic crystal field. In this study we present quantitative evidence in support of this interpretation and also include our work on Eu_2CuO_4 and Sm_2CuO_4, which are special cases because the multiplet intervals for Eu^{3+} and Sm^{3+} are not large compared to thermal energies. Below we present the results of magnetic susceptibility measurements on these compounds and their interpretation.

TABLE I

MAGNETIC PARAMETERS IN Ln_2CuO_4

Compound	$\mu_J(\beta)^a$	$\mu'(\beta)^b$	$\mu(\beta)^c$	$\Theta(K)^d$
Pr_2CuO_4	3.58	3.59	3.62	−97
Nd_2CuO_4	3.63	3.62	3.80	−4
Gd_2CuO_4	7.94	7.79	8.20	−15[d]

[a] μ_J is the magnetic moment of Ln^{3+} calculated by assuming that the multiplet separation between levels having different J values is large compared to the thermal energy kT, but the kT is large compared to the crystal-field splitting of the lowest multiplet level. In this case $\mu_J = g\beta\,[J(J+1)]^{1/2}$ and $g = 1 + [J(J+1) + S(S+1) - L(L+1)]/2J(J+1)$ (*11*).

[b] μ' is the experimental magnetic moment for the corresponding lanthanide trifluorides (*10*).

[c] μ and Θ are the experimental magnetic moment and Weiss constant, respectively.

[d] From the strong exchange narrowing of the Gd^{3+} EPR signal in Gd_2CuO_4 (*9*), we have estimated that $|\Theta| \approx 12$ K.

Experimental

The Ln_2CuO_4 samples were prepared by firing stoichiometric amounts of high-purity Ln_2O_3 (99.99%) and CuO (99.999%) in flowing oxygen at 1100°C for 48 hr with an interruption for regrinding. Ln_2O_3 was heated overnight at 1000°C in flowing oxygen before the reaction to remove moisture and CO_2. Attempts to obtain analogous compounds with Y, Dy, Er, and Yb were unsuccessful and resulted in mixtures of $Ln_2Cu_2O_5$ and Ln_2O_3. Although no attempt was made to ascertain the oxygen stoichiometry, studies of the $La_{2-x}Sr_xCoO_4$ (*12*) system suggest that these compounds are nearly stoichiometric (O_{4+x}, where $x \lesssim \pm 0.1$).

Powder X-ray diffraction was used to verify that all samples subjected to magnetic investigation were single phase. Cell constants were determined with a Guinier camera using copper $K\alpha$ radiation and a least-squares refinement program (*13*) and were found to be in good agreement with previous work (*4*, *6–8*).

Magnetic susceptibility measurements were made in the range 4.2–300 K using a Faraday apparatus described elsewhere (*14*). The setup was calibrated with palladium (NBS No. 765). The maximum field was about 12.5 kG, with $HdH/dz \approx 13$ (kG)^2 cm^{-1}. χ was measured at six field strengths ranging from 7.5 to 12.5 kG at each temperature. Since χ was independent of field at all temperatures, the reported values represent the average of six measurements at each temperature. The susceptibilities were corrected for ionic diamagnetism using the values -16×10^{-6} emu/mole for O^{2-}, -11×10^{-6} emu/mole for Cu^{2+}, and -20×10^{-6} emu/mole for Ln^{3+} (*15*). Theoretical fits to the experimental susceptibilities were performed using a Hewlett–Packard 9810 calculator.

EPR measurements were performed at ambient temperature using an IBM ER 200 D spectrometer.

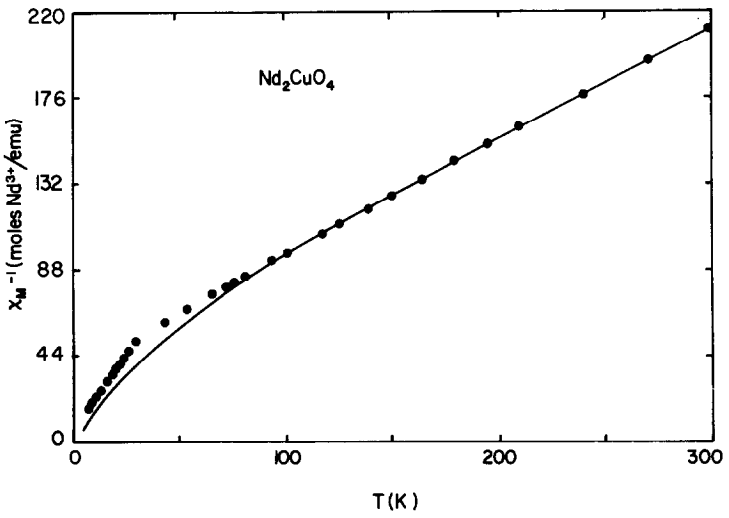

FIG. 3. Temperature dependence of the reciprocal magnetic susceptibility of Nd_2CuO_4 per mole of Nd^{3+}. The dots are experimental values, and the solid line represents the bets fit to Eq. (3) to the experimental data at elevated temperatures.

Results

Nd_2CuO_4

The temperature dependence of the reciprocal magnetic susceptibility of Nd_2CuO_4 per mole of Nd^{3+} is shown in Fig. 3. The reciprocal susceptibility obeys the Curie–Weiss law, $\chi^{-1} = (T - \theta)/C$, above about 30 K, and the magnetic moment evaluated from the slope of the χ^{-1} vs T plot is in very good agreement with that for Nd^{3+} only (see Table I). A break in the χ^{-1} vs T plot occurs near 30 K, and below this temperature a second Curie–Weiss law appears to be followed. Cu^{2+}, whose magnetic moment usually lies in the range 1.8–2.2 β (*16*), apparently does not contribute to χ because the Cu^{2+} ions are coupled antiferromagnetically in the CuO_2 planes. Our failure to observe a Cu^{2+} EPR signal at 300 K (*9*) confirms the antiferromagnetic alignment of the Cu^{2+} moments. No EPR signal for Nd^{3+} was observed due to the large orbital component of its magnetic moment, which results in rapid magnetic relaxation and EPR signals that are normally too broad to observe, except perhaps at very low temperatures.

Since Cu^{2+} apparently does not contribute to χ, we have attempted to understand the temperature dependence of χ on the basis of that of Nd^{3+} alone. In Nd_2CuO_4, Nd^{3+} is surrounded by a nearly cubic array of oxygen ligands (see Fig. 2), with four oxygens located at a distance of 2.32 Å and the other four positioned at 2.68 Å. Hence, in a first approximation, we assume that the crystalline electric field at the Nd^{3+} site has cubic symmetry, so that the theoretical expressions of Penney and Schlapp (*17*) can be used to fit the data. The latter authors found that the ground state of $Nd^{3+}(4f^3)$, which is $^4I_{9/2}$, would split into three levels in a cubic field, with the upper two being doubly degenerate, so that there would be further splitting if the ligand symmetry were lower than cubic. The solution of their secular determinent gives the following equations for the ten energy levels in the presence of a magnetic field:

$$W_1 = 20.95\ A + 1.833\ G + 0.3879\ G^2/A,$$

$$W_2 = 9.11\,A + 2.788\,G - 0.3411\,G^2/A,$$
$$W_3 = 9.11\,A - 0.542\,G + 0.1015\,G^2/A,$$
$$W_4 = -19.59\,A - 3.121\,G - 0.00468\,G^2/A,$$
$$W_5 = -19.59\,A + 1.542\,G - 0.1015\,G^2/A, \quad (1)$$

and the five remaining levels can be generated by changing the sign of G. In Eq. (1), the constant A is proportional to the cubic field constant D, which enters into the cubic crystalline electric field potential $V = D(x^4 + y^4 + z^4)$, and $G = g\beta H$, where g is the g factor ($g = 8/11$ for Nd^{3+}), β is the Bohr magneton, and H is the applied magnetic field. The magnetic susceptibility per mole of Nd^{3+} can then be calculated using the general expression (*18*)

$$\chi_m = \frac{N_0}{H}\sum_i \frac{\partial W_i}{\partial H} \exp(-W_i/kT) \Big/ \sum_i \exp(-W_i/kT) \quad (2)$$

where N_0 is Avagadro's number and the summation extends over all levels in the multiplet given by Eq. (1). Using Eqs. (1) and (2), we have verified that the suceptibility per mole of Nd^{3+} is given by

$$\chi_M(Nd^{3+}) = (2g^2\beta^2N_0/A)[(0.1483e^{19.59\alpha} + 0.2396e^{-9.11\alpha} - 0.3879e^{-20.95\alpha}) + \alpha(6.065e^{19.59\alpha} + 4.031e^{-9.11\alpha} + 1.680e^{-20.95\alpha})] \div (2e^{19.59\alpha} + 2e^{-9.11\alpha} + e^{-20.95\alpha}), \quad (3)$$

where $\alpha = A/kT$ (*17*). The above expression for the susceptibility is valid under three conditions: (1) the crystal field has cubic symmetry, (2) the thermal occupation of higher multiplet levels can be neglected,[1] and (3) exchange interactions involving the lanthanide ions are unimportant.

It is noteworthy that Eq. (3) reduces to the Curie law, $\chi = C/T$, at sufficiently high temperatures ($\alpha \to 0$), but at intermediate temperatures, where kT is of the same order as the energy-level separations produced by the crystal field, the susceptibility follows the Curie–Weiss law, $\chi = C/T(-\theta)$, over a wide range of temperatures. At sufficiently low temperatures ($\alpha \to \infty$), χ deviates from the Curie–Weiss law and displays a Curie law characteristic of the magnetic ground state of Nd^{3+}. To fit Eq. (3) to the experimental data for Nd_2CuO_4, it is only necessary to determine the best value of the constant A. Since our data cover the intermediate and low-temperature regions, the most reliable method for evaluating A is to fit the experimental data at elevated, rather than low, temperatures to avoid possible impurity contributions to the susceptibility. The best fit of Eq. (2) to the experimental data is shown in Fig 3, and the resulting value of A is -28.5 cm^{-1}. Using Eq. (1), the splitting of the lowest multiplet level is shown in Fig. 4.

Pr_2CuO_4

The reciprocal susceptibility of Pr_2CuO_4 per mole of Pr^{3+} vs temperature is displayed in Fig. 5. As found in Nd_2CuO_4, the susceptibility at temperatures above about 65 K obeys the Curie–Weiss law, and the experimental magnetic moment is in excellent agreement with that for Pr^{3+} alone (see Table I). A weak Cu^{2+} EPR signal characteristic of Cu^{2+} in an axially distorted site ($g_\parallel = 3.00$, $g_\perp = 2.27$) has been observed at 300 K (*9*), which is probably due to a small quantity of an impurity phase. Again, no Pr^{3+} EPR signal could be detected due to its large orbital moment.

Below about 65 K, χ^{-1} begins to flatten out, and, in analogy to Nd_2CuO_4, we have attempted to fit the variation of χ with temperature assuming that Pr^{3+} is located in a

[1] Since the multiplet separation between the ground multiplet ($J = 9/2$) and first excited multiplet ($J = 11/2$) is about 1800 cm^{-1}, correction to the susceptibility due to the thermal occupation of the $J = 11/2$ multiplet at 300 K is only about three percent (*17*).

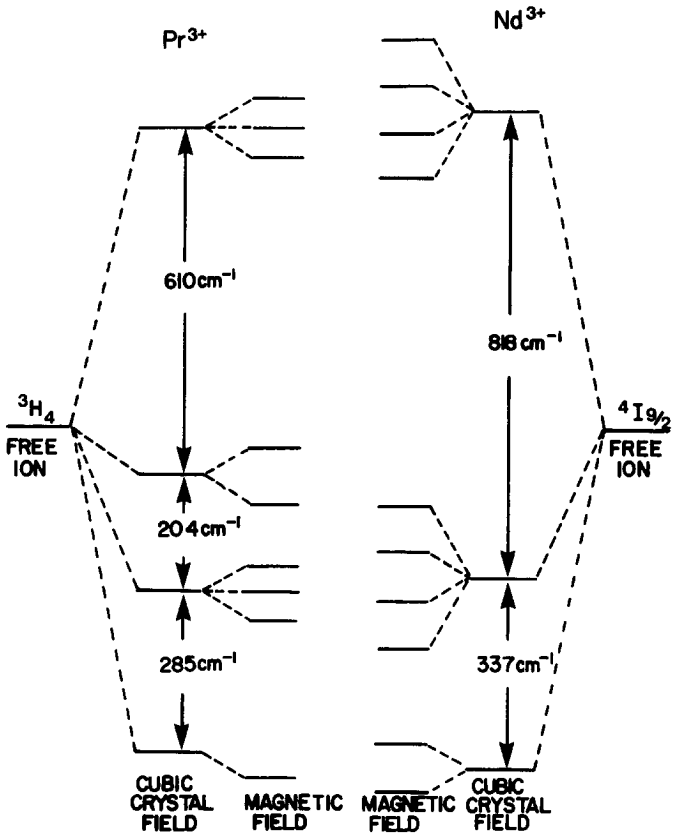

FIG. 4. Splitting of the lowest multiplet level for Nd^{3+} and Pr^{3+} in Nd_2CuO_4 and Pr_2CuO_4 derived by fitting Eqs. (3) and (5), respectively, to the experimental susceptibility data at elevated temperatures.

cubic field of oxygen ligands. For this case Penney and Schlapp (*17*) have shown that the $^3H_4$ ground multiplet of $Pr^{3+}(4f^2)$ splits into four levels, and their expressions[2] for the nine resulting energy levels in the presence of a magnetic field are given below:

$$W_1 = 672a + 5G^2/252a,$$
$$W_2 = 336a + G/2 + 7G^2/3840a,$$
$$W_3 = 336a + 2G^2/105a,$$
$$W_4 = 336a - G/2 + 7G^2/3840a,$$
$$W_5 = 96a + G^2/180a,$$
$$W_6 = 96a - G^2/180a,$$
$$W_7 = -624a + 5G/2 - 7G^2/3840a,$$
$$W_8 = -624a - G^2/180a,$$
$$W_9 = -624a - 5G/2 - 7G^2/3840a; \quad (4)$$

where a is proportional to the cubic field constant D and $G = g\beta H$ ($g = 4/5$ for Pr^{3+}). Using Eqs. (2) and (4), the calculated susceptibility per mole of Pr^{3+} can be written

$$\chi_M(Pr^{3+}) = (2N_0g^2\beta^2/a)[53e^{13\beta}/5760 + e^{-2\beta}/30 - 61e^{-7b}/2688 - 5e^{-14\beta}/252 + \beta(25e^{13\beta} + e^{-7\beta})/192] \div (3e^{13\beta} + 2e^{-2\beta} + 3e^{-7b} + e^{-14\beta}), \quad (5)$$

where $\beta = 48a/kT$. Equation (5) is valid un-

[2] We have corrected an error in their equation for W_6.

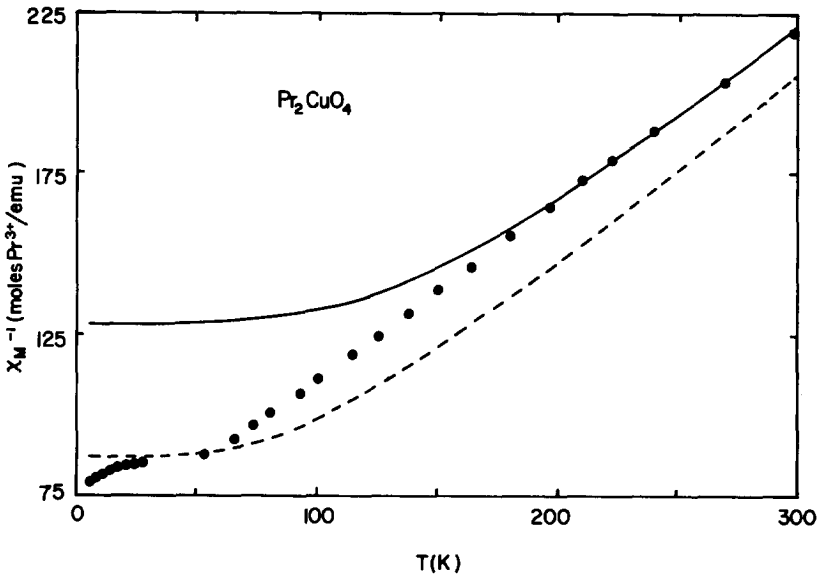

FIG. 5. Temperature dependence of the reciprocal magnetic susceptibility of Pr_2CuO_4 per mole of Pr^{3+}. The dots are experimental values, and the solid and dashed lines represent the best fits of Eq. (5) to the experimental data at elevated and low temperatures, respectively.

der the same conditions as Eq. (3)[3] and also exhibits the same temperature regimes. Figure 5 shows the best fits of Eq. (5) to the experimental data derived by fitting the data at both low and elevated temperatures, and the corresponding values of a are -0.572 and -0.848 cm^{-1}, respectively. As discussed in connection with Nd_2CuO_4, the latter value of a is probably the most reliable. Taking $a = -0.848$ cm^{-1} and using Eq. (4), the splitting of the lowest multiplet level is depicted in Fig. 4.

Eu_2CuO_4

The temperature dependence of the magnetic susceptibility of Eu_2CuO_4 per mole of Eu^{3+} is shown in Fig. 6. χ increases with decreasing temperature down to about 100 K, below which it flattens out. Eu^{3+} has an electronic configuration $4f^6$, which gives rise to seven energy levels $^7F_0$, $^7F_1$, $^7F_2$, $^7F_3$, $^7F_4$, $^7F_5$, and $^7F_6$, with ^7F being the ground state. Eu^{3+} is particularly interesting because the energy-level differences are usually comparable to kT at elevated temperatures, so that the effect of temperature on the magnetic susceptibility is much more pronounced in Eu^{3+} than for the other trivalent lanthanide ions. Assuming Russell-Saunders coupling, the energy levels of the multiplets can be written (*19*)

$$W_J = \frac{\lambda}{2}[J(J+1) - L(L+1) - S(S+1)] + C, \quad (6)$$

where λ is the spin–orbit coupling constant, and C is a constant which is independent of J. Van Vleck (*20*) has shown that the susceptibility per mole of Eu^{3+} is given by

$$\chi_M(Eu^{3+}) = (0.1241/\gamma T)[24 + (13.5\gamma - 1.5)e^{-\gamma} + (67.5\gamma - 2.5)e^{-3\gamma} + (189\gamma - 3.5)e^{-6\gamma} + \ldots] \div (1 + 3e^{-\gamma} + 5e^{-3\gamma} + 7e^{-6\gamma} + \ldots), \quad (7)$$

[3] Since the separation between the $J = 4$ and $J = 5$ levels for Pr^{3+} is about 2100 cm^{-1} (*17*), thermal occupation of the higher levels may be neglected in calculating the susceptibility.

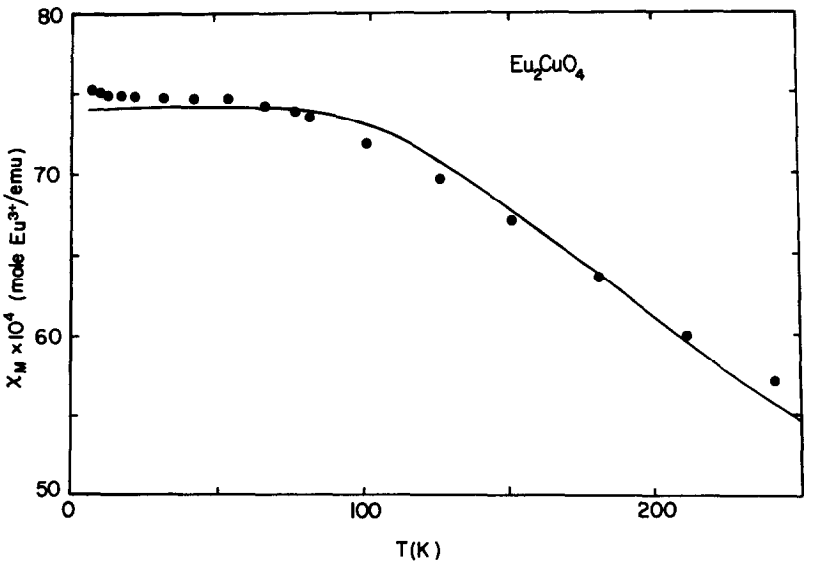

FIG. 6. Temperature dependence of the magnetic susceptibility of Eu_2CuO_4 per mole of Eu^{3+}. The dots are experimental values, and the solid line represents the best fit of Eq. (7) to the experimental data at elevated temperatures.

where γ is 1/21 of the ratio of the overall multiplet width to kT, i.e., $\gamma = \lambda/kT$. The best fit of Eq. (7) to the experimental data at elevated temperatures is shown in Fig. 6, for which λ has the value 280 cm^{-1}. Using Eq. (6), the multiplet splittings are shown in Fig. 7. Although the overall multiplet width is large compared to kT, the separation between the $J = 0$ and $J = 1$ levels is comparable to kT at ambient temperature (kT at 300 K = 209 cm^{-1}), which necessitates our use of the more accurate intermediate expression given by Eq. (7).

Sm_2CuO_4

The variation of the magnetic susceptibility of Sm_2CuO_4 with temperature is shown in Fig. 8. χ is nearly independent of temperature and displays a maximum at 7.6 K. Sm^{3+} has an electronic configuration $4f^5$ and, in order of increasing energy, the energy levels are $^6H_{5/2}$, $^6H_{7/2}$, $^6H_{9/2}$, $^6H_{11/2}$, etc. Like Eu^{3+}, the separation of these energy levels is normally not very large compared to kT. In the Russell-Saunders scheme, the energy levels are given theoretically by Eq. (*6*), and Van Vleck (*20*) has shown that the resulting susceptibility per mole of Sm^{3+} is given by

$$\chi_M(Sm^{3+}) = (0.1241/\delta T)[2.14\delta + 3.67 + (42.9\delta + 0.82)e^{-7\delta} + (142\delta - 0.33)e^{-16\delta} + \ldots] \div (3 + 4e^{-7\delta} + 5e^{-16\delta} + \ldots), \quad (8)$$

where δ is 1/55 of the ratio of the overall multiplet width to kT, i.e., $\delta = 27\lambda/110\ kT$. The best fit of Eq. (8) to the experimental data at elevated temperatures is shown in Fig. 8, and the best-fit value of λ is 296 cm^{-1}. The resulting multiplet splittings derived from Eq. (6) are shown in Fig. 7, where it can be seen that the separation between the $J = 5/2$ and $J = 7/2$ levels is not very large compared to kT at ambient temperature, which again justifies our use of the intermediate formula given by Eq. (8).

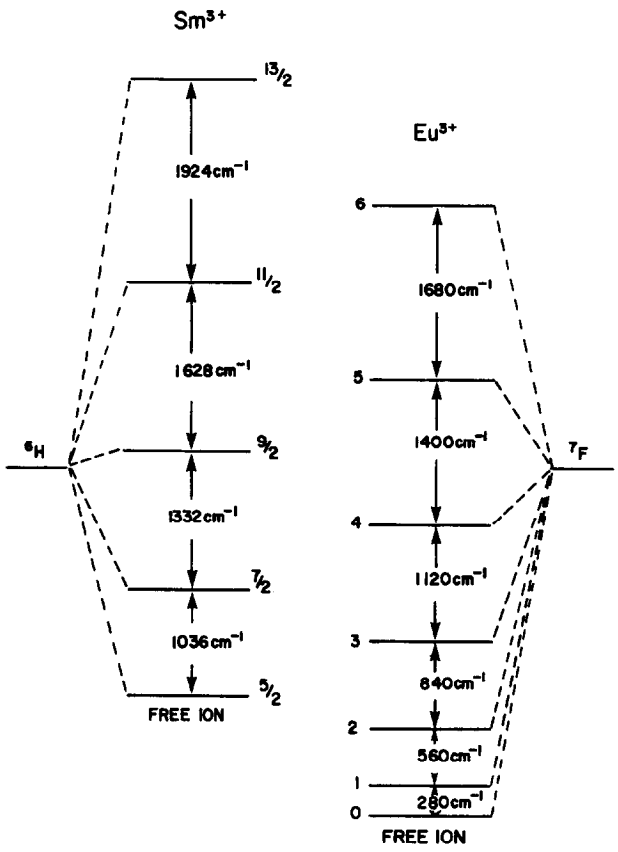

FIG. 7. Multiplet splittings for Eu^{3+} and Sm^{3+} in Eu_2CuO_4 and Sm_2CuO_4 derived by fitting Eqs. (7) and (8) to the experimental susceptibility data at elevated temperatures.

Discussion

First we consider the agreement between theory and experiment and then proceed to a discussion of the parameters derived by fitting Eqs. (3), (5), (7), and (8) to the experimental data.

For Nd_2CuO_4 and Eu_2CuO_4, the agreement between the experimental susceptibility and that calculated using Eqs. (3) and (7) is very good over the entire temperature range (see Figs. 3 and 6), which supports the assumptions used in calculating the susceptibilities of these compounds. Their magnetic behavior can be understood on the basis of the trivalent lanthanide contribution only without invoking exchange interactions either between the lanthanide ions or between the lanthanide and cupric ions. The absence of a Cu^{2+}-ion contribution to χ below 300 K provides definitive evidence that these ions are ordered antiferromagnetically in the CuO_2 planes of these compounds.

Qualitatively, the variation of χ with temperature for Nd_2CuO_4 and Eu_2CuO_4 can be understood by reference to the energy-level diagrams in Figs. 4 and 7, respectively. In Nd_2CuO_4, χ changes from the Curie–Weiss law at intermediate temperatures ($300 \gtrsim T \gtrsim 30$ K) to a near-Curie law at low temperatures ($T \lesssim 30$ K) due to occupation of magnetic ground and excited states of Nd^{3+}. Although theoretically a Curie law should be

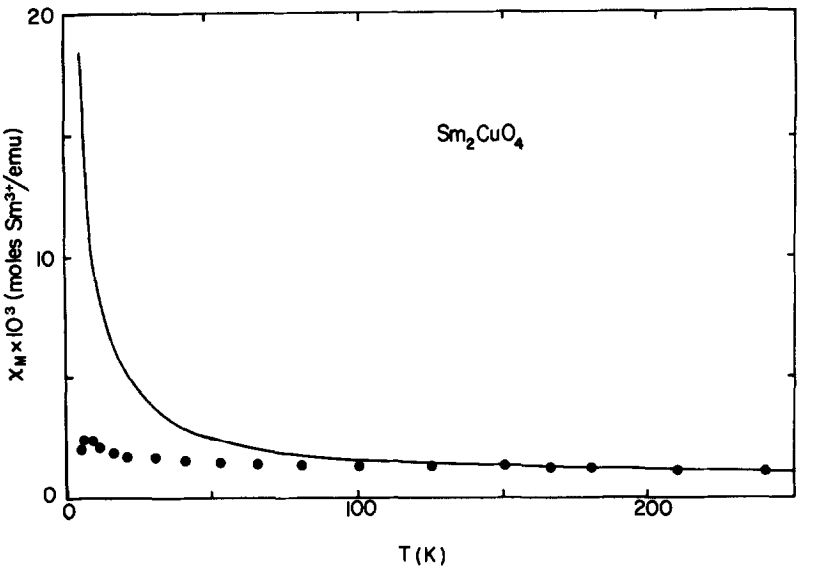

FIG. 8. Temperature dependence of the magnetic susceptibility of Sm_2CuO_4 per mole of Sm^{3+}. The dots are experimental values, and the solid line represents the best fit of Eq. (8) to the experimental data at elevated temperatures.

obeyed at very low temperatures, at sufficiently low temperatures even the relatively weak exchange interactions involving Nd^{3+} will be manifested. Our finding that $\Theta \approx -4$ K, which is the lowest temperature attained in these experiments, indicates that the Nd^{3+} exchange interactions are antiferromagnetic and is consistent with $\Theta \approx -15$ K and $T_N \approx 5$ K for Gd_2CuO_4 (*9*). In Eu_2CuO_4, the Eu^{3+} excited states are magnetic and their occupation at elevated temperatures produces a paramagnetic susceptibility. However, the Eu^{3+} ground state is nonmagnetic, which causes χ to become independent of temperature at lower temperatures ($T \lesssim 100$ K).

For Pr_2CuO_4 and Sm_2CuO_4, the agreement between Eqs. (5) and (8) and experiment is excellent above about 150 and 100 K, respectively. In Pr_2CuO_4, the experimental χ is larger than that predicted by fitting the data to Eq. (5) at elevated temperatures (≈35% difference at 25 K; see Fig. 5), although both curves display the same qualitative features. The flattening of χ at low temperatures follows from the energy-level diagram in Fig. 4, since the excited states of Pr^{3+} are magnetic, whereas the ground state is nonmagnetic. Moreover, taking the less physical approach of fitting the data at low, rather than high, temperatures results in a 6% negative deviation from the Curie–Weiss law (see Fig. 5). However, it should be pointed out that the crystal structure of Pr_2CuO_4 has not been determined, so that structural differences between Nd_2CuO_4 and Pr_2CuO_4, and particularly those involving the Ln^{3+} site, may be the origin of the discrepancy between theory and experiment. Although preliminary calculations for a crystalline field of rhombic symmetry yield better agreement with experiment, it is premature to present the results of these calculations in view of our lack of knowledge of the structure of Pr_2CuO_4. Moreover, it has been found that the low-temperature susceptibility of the praseodymium oxides is strongly dependent on oxygen stoichiometry (*21*), with χ_M^{-1} decreasing by about 40% in going from $PrO_{1.50}$

to $PrO_{1.556}$ and exhibiting the same qualitative negative deviation from the data fitted at elevated temperatures as found for Pr_2CuO_4 in Fig. 5. It is also possible that ferromagnetic interactions between the Pr^{3+} moments may play a role in increasing the experimental susceptibility below 150 K.

In contrast to Pr_2CuO_4, the experimental susceptibility of Sm_2CuO_4 below 100 K is smaller than that predicted by fitting Eq. (8) to the data at elevated temperatures. The predicted Curie-law behavior at low temperatures results from the occupation of the magnetic ground level depicted in Fig. 7. The reduction in χ and maximum in χ near 7.6 K suggests that antiferromagnetic interactions involving the Sm^{3+} moments are probably operative. Although the susceptibility maximum near 7.6 K in Sm_2CuO_4 is in reasonable accord with $T_N \approx 5$ K in Gd_2CuO_4 and $\Theta \approx -4$ K in Nd_2CuO_4, this compound exhibits by far the largest deviation from the predicted behavior at low temperatures. Since the crystal structure of Sm_2CuO_4 has not been determined, any structural differences between Sm_2CuO_4 and Nd_2CuO_4 could play an important role in explaining the large discrepancy between experiment and theory at low temperatures. Moreover, it is difficult to envision how low levels of impurities and/or oxygen nonstoichiometry can account for the nearly temperature independent susceptibility of Sm_2CuO_4 at low temperatures. Also, in both Pr_2CuO_4 and Sm_2CuO_4 there is no evidence of a Cu^{2+}-ion contribution of χ below 300 K, so that again the cupric ions appear to be ordered antiferromagnetically in the CuO_2 planes of these compounds.

The susceptibility parameters for Nd_2CuO_4, Pr_2CuO_4, Eu_2CuO_4, and Sm_2CuO_4, derived by fitting Eqs. (3), (5), (7), and (8), respectively, to the experimental data, are summarized in Table II. Using the theory of Penney and Schlapp (*17*), the ratio of the cubic field constants of Nd^{3+} and Pr^{3+} is given by the expression

TABLE II

SUSCEPTIBILITY PARAMETERS FOR LANTHANIDE IONS

Ion	Parameter (cm^{-1})[a]	Parameter (cm^{-1})
Nd^{3+}	−28.5	−20.6[c]
Pr^{3+}	−0.848 (−0.572)[b]	−0.293[c]
Eu^{3+}	280	291 (240; 320)[d]
Sm^{3+}	296	306 (240; 294)[d]

[a] This work. The parameters listed are A and a for Nd^{3+} and Pr^{3+} in Nd_2CuO_4 and Pr_2CuO_4, respectively, and λ for Eu_2CuO_4 and Sm_2CuO_4. These parameters were derived by fitting Eqs. (3), (5), (7), and (8) to the susceptibility data at elevated temperatures.

[b] The value in parentheses was derived by fitting Eq. (5) to the low-temperature susceptibility data for Pr_2CuO_4.

[c] Other works. A and a were derived by fitting Eqs. (3) and (5) to the susceptibility data for $Nd_2(SO_4)_3 \cdot 8H_2O$ and $Pr_2(SO_4)_3 \cdot 8H_2$), respectively (*17*).

[d] Values derived using $\sigma = 33$ (24). Values in parentheses are calculated for pure Russel-Saunders coupling (first number) and for Russel-Saunders coupling corrected to second order to include the effects of spin–orbit coupling (second number) (*26*).

$$D_{Nd}/D_{Pr} = Ap_4/12\sqrt{14}\, aP_{9/2}, \qquad (9)$$

where p_4 and $p_{9/2}$ are the matrix-element coefficients of the crystal field, with $p_4 = -21\ I_{Pr}/11(10{,}395)$ and $p_{9/2} = -2{,}380\ I_{Nd}/1{,}001(32{,}670)$. Here $I = \int_0^\infty r^6 R^2(r)dr$, where $R(r)$ is the radial wavefunction of the $4f$ electrons. Substituting the values of A, a, p_4, and $p_{9/2}$ into Eq. (9), we find $D_{Nd}/D_{Pr} = 2.80\ I_{Pr}/I_{Nd}$ for $a = -0.572$ cm^{-1} and $D_{Nd}/D_{Pr} = 1.89\ I_{Pr}/I_{Nd}$ for $a = -0.848$ cm^{-1}. Since the integral I depends only upon the principal quantum number n of the $4f$ electrons and the effective nuclear charge $(Z - \sigma)$, where Z is the atomic number and σ is the screening constant, we expect the ratio $I_{Pr}/I_{Nd} \approx 1$. However, this integral ratio can be estimated by using hydrogenic $4f$ radial wavefunctions, which have the form $R(r) = Br^{n-1}e^{-(Z-\sigma)r/na_0}$, where B is a normalization constant and a_0 is the Bohr radius. In this case, evaluation of the integral ratio yields $I_{Pr}/I_{Nd} = [(Z_{Pr} - \sigma)/(Z_{Nd} - \sigma)]^{12.4}$. σ can be

determined from the theoretical overall multiplet width, which is given by (*22*)

$$\Delta W \frac{5.82(2L + 1)}{n^3 l(l + 1)(2l + 1)} (Z - \sigma)^4, \quad (10)$$

where ΔW is in cm^{-1} and l is the azimuthal quantum number. Substitution of the overall multiplet widths for Eu^{3+} or Sm^{3+} into Eq. (10) yields $\sigma = 33$, which is in good agreement with values derived from X-ray data (*23*) and also from less detailed magnetic measurements on other trivalent europium and smarium compounds (*24*). Hence we estimate that $D_{Nd}/D_{Pr} = 1.75$ and 1.18 cm^{-1} for $a = -0.572$ and -0.848 cm^{-1}, respectively. These values are in reasonable agreement with the expectation that the crystalline electric fields at the Nd^{3+} and Pr^{3+} sites have quite similar magnitudes, which verifies the internal consistency of this magnetic approach to the determination of crystal field parameters. However, in view of the approximations involved in this procedure, it is not possible to conclude that Nd^{3+} and Pr^{3+} are located at identical sites in these compounds. In this regard, it should be mentioned that in previous magnetic susceptibility studies of $Nd_2(SO_4)_3 \cdot 8H_2O$ and $Pr_2(SO_4)_3 \cdot 8H_2O$ (*17*) there was nearly perfect agreement between experiment and Eqs. (3) and (5) using the susceptibility parameters given in Table II. However, it was found that $D_{Nd}/D_{Pr} \approx 4$, which seems unreasonable when one considers the high degree of structural and chemical similarity between these two compounds. This discrepancy is primarily due to uncertainties in the experimental data for the neodymium compound. Subsequent spectroscopic measurements (*25*) of the energy levels of $Nd_2(SO_4)_3 \cdot 8H_2O$ yielded $D_{Nd}/D_{Pr} \approx 1.3$, which is in fair agreement with our estimate of this ratio.

[4] The assumption of a hydrogenic $4f$ radial wavefunction to calculate the integral ratio should be a good approximation, since this ratio is relatively insensitive to the shape of the wavefunction.

Finally, the parameters for Eu^{3+} and Sm^{3+} given in Table II are in good agreement with the free-ion values derived by Van Vleck (*24*) using $\sigma \approx 33$ to fit the susceptibility data for europium and samarium oxides and sulfates. Table II also shows that these parameters are in fair agreement with those calculated from Judd's (*26*) theoretical energy levels for pure Russel-Saunders coupling and for Russel-Saunders coupling corrected to second order to include the effects of spin–orbit coupling.

In summary, we have found that the magnetic behavior of these semiconducting Ln_2CuO_4 compounds is relatively simple, in the sense that the Cu^{2+} ions are ordered antiferromagnetically in the CuO_2 planes of these compounds and the exchange interactions involving the Ln^{3+} ions are relatively weak, so that the magnitude and temperature dependence of the susceptibility at elevated temperatures are in excellent agreement with the predicted behavior for isolated Ln^{3+} ions under the influence of a cubic crystal field. Hence these compounds form an interesting new series of planar Cu^{2+}-ion antiferromagnets. The antiferromagnetic Cu^{2+}–O^{2}–Cu^{2+} superexchange interaction probably involves overlap of the Cu^{2+}-ion $3d_{x^2-y^2}$ orbital with the O^{2-}-ion $2p_x$ and $2p_y$ orbitals (*9, 27*), where the x, y, and z axes are directed along the Cu^{2+}–O^{2-} bonds, with the z axis lying perpendicular to the CuO_2 planes shown in Figs. 1 and 2. To further elucidate the nature of the Cu^{2+} magnetic ordering in these compounds, we are currently undertaking neutron diffraction experiments to explore their magnetic structures as well as high-temperature susceptibility measurements to determine their Néel temperatures. It would also be of interest to verify spectroscopically the magnetically derived energy-level separations shown in Figs. 4 and 7.

Acknowledgments

The authors acknowledge the Center for Solid State

Science at Arizona State University for use of its facilities. They also thank Dr. J. M. Longo for valuable discussions.

References

1. R. J. Birgeneau, J. Shalo, Jr., and G. Shirane, *J. Appl. Phys.* **41,** 1303 (1970).
2. P. Ganguly and C. N. R. Rao, *Mater. Res. Bull.* **8,** 405 (1973).
3. T. Kenyo and S. Yajima, *Bull. Chem. Soc. Japan* **46,** 1329 (1973).
4. J. M. Longo and P. M. Raccah, *J. Solid State Chem.* **6,** 526 (1973).
5. R. Saez Puche, M. Norton, and W. S. Glaunsinger, *Mater. Res. Bull.*, in press.
6. I. S. Shaplygin, B. G. Kakhan, and V. B. Lazarev, *Russ. J. Inorg. Chem.* **24,** 820 (1979).
7. V. B. Grande, H. Müller-Buschbaum, and M. Schweizer, *Z. Anorg. Allg. Chem.* **428,** 120 (1977).
8. H. Müller-Buschbaum and W. Wollschläger, *Z. Anorg. Allg. Chem.* **414,** 76 (1975).
9. R. Saez Puche, M. Norton, and W. S. Glaunsinger, *Mater. Res. Bull.* **17,** 1523 (1982).
10. S. Kern and P. M. Raccah, *J. Phys. Chem. Solids* **26,** 1625 (1965).
11. J. H. Van Vleck, "The Theory of Electric and Magnetic Susceptibilities," p. 232, Oxford Univ. Press, London (1965).
12. P. Ganguly and S. Ramasesha, *Magn. Lett.* **1,** 131 (1980).
13. D. E. Appleman and H. T. Evans, Jr., Indexing and Least Squares Refinement of Powder Diffraction Data, Report USG-GD-73-003 (1973).
14. M. Mobley, Ph.D. thesis, Arizona State University (1977).
15. L. N. Mulay, "Magnetic Susceptibility," p. 1782, Wiley, New York (1963).
16. Ref. (*11*), p. 285.
17. W. G. Penney and R. Schlapp, *Phys. Rev.* **41,** 194 (1932).
18. Ref. (*11*), p. 181.
19. Ref. (*11*), p. 236.
20. Ref. (*11*), p. 248.
21. S. Kern, *J. Chem. Phys.* **40,** 208 (1964).
22. Ref. (*11*), p. 238.
23. G. Wentzel, *Z. Phys.* **33,** 849 (1925).
24. Ref. (*11*), p. 251.
25. F. H. Spedding, *J. Chem. Phys.* **1,** 316 (1937).
26. B. R. Judd, *Proc. Phys. Soc. (London) A69,* 157 (1956).
27. J. B. Goodenough, *Mater. Res. Bull.* **8,** 423 (1973).